


Received: 17 December 2021

Revised: 30 January 2022

Accepted: 31 January 2022

Enzyme based field effect transistor: State-of-the-art and future perspectives

Lucia Sarcina¹ | Eleonora Macchia² | Angelo Tricase¹ | Cecilia Scandurra¹ | Anna Imbriano^{1,3} | Fabrizio Torricelli⁴ | Nicola Cioffi^{1,3} | Luisa Torsi^{1,2,3} | Paolo Bollella^{1,3} 

¹Dipartimento di Chimica, Università degli Studi di Bari "Aldo Moro", Bari, Italy

²Faculty of Science and Engineering, Åbo Akademi University, Turku, Finland

³Centre for Colloid and Surface Science - Università degli Studi di Bari "Aldo Moro", Bari, Italy

⁴Dipartimento Ingegneria dell'Informazione, Università degli Studi di Brescia, Brescia, Italy

Correspondence

Luisa Torsi and Paolo Bollella, Dipartimento di Chimica, Università degli Studi di Bari "Aldo Moro", 70125 Bari, Italy.

Email: luisa.torsi@uniba.it and paolo.bollella@uniba.it

Abstract

The review discloses the historical and technological evolution of enzyme-based field-effect transistors (EnFETs) underlying the importance of gate electrode modification toward the implementation of novel FETs configurations such as extended-gate FET (EG-FETs) or EG organic FETs (EG-OFETs). The working principle of the EnFETs as postulated by Bergveld in 1970, who defined the EnFET as an ion-selective FET (ISFET) modified with enzyme-membrane, is also discussed considering the analytical equations related to the EnFET output response. For each category, namely EnFETs, EG-FETs, and EG-OFETs, we reviewed the key devices' configurations that addressed the research in this field in the last 40 years with particular attention to the analytical figures of merit.

KEYWORDS

enzymes, extended gate configuration, field-effect transistors, modified electrodes, potentiometric sensors

Abbreviations: ADH, alcohol dehydrogenase; APOA1, Apolipoprotein A1; AZO, aluminium-zinc-oxide; BAC, blood alcohol content; ChEs, cholinesterases; DET, direct electron transfer; DG, dual-gate; EG-FETs, extended-gate FET; EG-OFETs, extended-gate organic FETs; ELISA, enzyme-linked immunosorbent assays; ENFETs, enzyme-based field-effect transistors; ET, electron transfer; FAD, flavin adenine dinucleotide; GOx, glucose oxidase; HRP, Horseradish peroxidase; ISFET, ion-selective field-effect transistor; LDH, lactate dehydrogenase; LOD, limit of detection; LOx, lactate oxidase; MOSFET, metal-oxide-semiconductor field-effect transistor; NAD⁺, nicotinamide dinucleotide; NADP⁺, nicotinamide adenine dinucleotide phosphate; OECTs, organic electrochemical transistors; ORP, osmium-redox polymer; OSCs, organic semiconductors; OTFTs, organic thin-film transistors; PB, Prussian blue; PEDOT:PSS, poly(3,4-ethylenedioxythiophene) doped with poly(styrenesulfonate); PEN, polyethylene naphthalate; PenFET, penicillinase modified FET; POx, pyranose oxidase; PQQ, pyrroloquinoline quinone; PS, polystyrene; SAM, self-assembled monolayer; SOI, silicon-on-insulator; EDC, 1-[3-(dimethylamino)propyl]-3-ethylcarbodiimide hydrochloride; ITO, indium tin oxide

1 | INTRODUCTION

Enzyme modified electrodes for the detection of metabolites have been widely investigated over the last six decades, considering both the amperometric transduction mechanism based on the detection of O₂/H₂O₂ as a first-generation electrode, and the potentiometric one based on the detection of H₂O₂ or H⁺ ions as chemical species inducing a variation in potential.^[1,2] Enzyme-based electrochemical biosensors are notoriously classified as (i) first-generation electrodes, where the enzymatic reaction is coupled with O₂ reduction to H₂O₂ enabling substrate quantification through the correlation with O₂ concentration monitored with Clark's electrode or through the correlation with H₂O₂, reduced to H₂O at the surface of a solid electrode (e.g., gold, graphite, etc. electrodes);^[3]

This is an open access article under the terms of the [Creative Commons Attribution](https://creativecommons.org/licenses/by/4.0/) License, which permits use, distribution and reproduction in any medium, provided the original work is properly cited.

© 2022 The Authors. *Electrochemical Science Advances* published by Wiley-VCH GmbH.

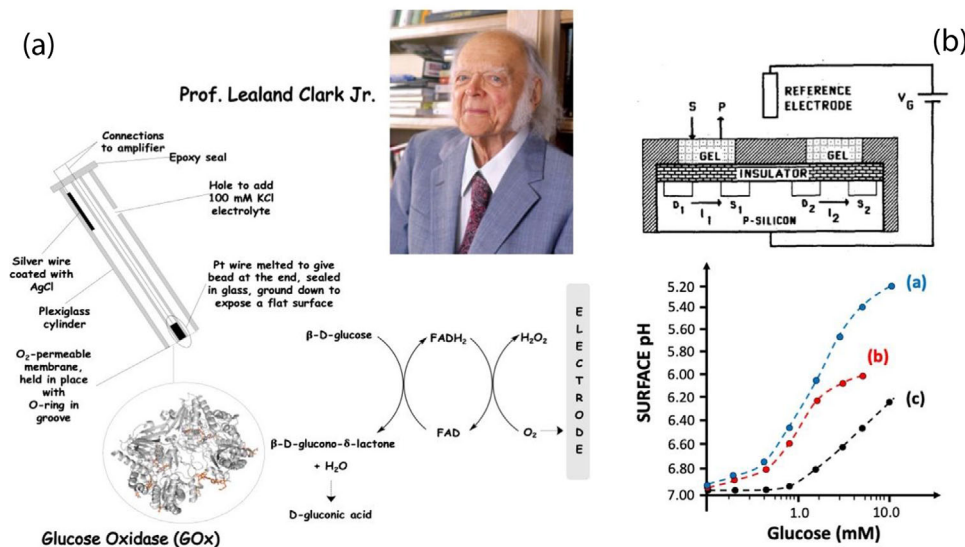


FIGURE 1 (a) Schematic representation of Clark's electrode to monitor O₂ variation modified with a glucose oxidase (GOx) membrane known as the first reported glucose biosensor (inset) picture of Prof. Leiland Clark Jr.; (b) Schematic representation of the first reported enzyme-based field-effect transistor (EnFET) for glucose detection where D and S are transistor drain and source, respectively. V_G is the applied gate voltage, and I is the drain-to-source current. The output curve measured as surface pH variation (local pH gradient) vs. glucose concentration for (a) 100% O₂ and 0.2 mM phosphate buffer, (b) 25% O₂ and 0.2 mM phosphate buffer, and (c) 100% O₂ and 1 mM phosphate buffer. The inset of Figure a is reproduced from https://en.wikipedia.org/wiki/File:Dr._Leland_C._Clark_Jr_2005.jpg under CC-BY-SA <https://creativecommons.org/licenses/by-sa/3.0/legalcode>. Figure 1b is adopted^[12] with permission of the American Chemical Society (ACS)

(ii) second-generation electrodes, where small electroactive molecules, known as diffusing (e.g., nicotinamide dinucleotide (NAD⁺) acting as a primary electron acceptor for NAD-dependent dehydrogenases that is catalytically re-oxidized by a catalyst) or immobilized mediators (e.g., ruthenium or osmium redox polymers), are shuttling electrons between the enzyme active center and the electrode;^[4,5] (iii) third generation electrodes, where enzymes are directly and electronically connected to the electrode (direct electron transfer [DET]).^[6–8] As a first-generation electrode, we should certainly highlight the work reported by Clark and Lyons in 1962, where glucose oxidase (GOx) was immobilized onto a semipermeable dialysis membrane deposited on the surface of Clark's electrode, monitoring O₂ consumption through the enzymatic oxidation of glucose, as reported in Figure 1a.^[9–11] Alternatively, the potentiometric detection of metabolites has been reported by using enzyme-modified ion-selective field-effect transistors (ISFET), where the enzyme is acting as a bioreceptor catalyzing two reactions, one sensing reaction (e.g., glucose oxidation, lactate oxidation, etc.) and a reaction producing a pH gradient at the interface, namely a variation of H⁺ concentration, detected by an ISFET.^[12] For instance, in 1985, Caras et al. developed a glucose potentiometric sensor based on a model to consider the effects of buffer, oxygen partial pressure, and time-response on the output signal.^[12] In this work, Caras and co-workers co-immobilized GOx from *Aspergillus*

niger and catalase onto a membrane deposited on the surface of an ISFET. Indeed, most of the ISFETs have been developed for the detection of H⁺ as pH sensors.^[13] Hence, GOx has been used to oxidize $\beta\text{-D-glucose}$ to gluconic acid that is undergoing deprotonation generating freely diffusing H⁺ (detected from the ISFET), while H₂O₂ is immediately decomposed to O₂ and H₂O by catalase, as displayed in Figure 1b. However, the aforementioned platform was inspired by an idea already conceived by Janata and Moss, in 1976, designing an enzyme-modified ISFET,^[14] and practically realized in 1980 developing a penicillin-responsive device.^[15] The latter was defined for the first time as an enzyme-based FET (EnFET).

This paper aims at reviewing the evolution of enzyme-based transistors both from a historical and technological point of view shedding the light on the gate electrode modification and its functionality toward the development of novel EnFETs. Herein, we will not extensively revise enzyme-based organic electrochemical transistors (OECTs) because they have been deeply reviewed elsewhere.^[16,17] Differently from previously proposed reviews on EnFETs,^[18,19] the focus here will be on the electron transfer (ET) mechanism correlated with the surface modification driving the detection of the analytical target. We will discuss separately EnFETs, extended-gate FETs (EG-FETs), and EG organic FETs (EG-OFETs) reported in the literature. In each section, we will highlight the key advantages/drawbacks of using a certain sensing architec-

ture focusing our attention on the gate detecting interface, including new possible effective modification strategies based on the knowledge of the ET pathway of enzymes. Indeed, we will consider two classes of enzymes accompanying the evolution of EnFETs, namely one directly producing the pH variation at the interface ion/selective membrane-insulator, as postulated by Bergveld in 1970, by means of H^+ variations or reactions products (e.g., NH_3 or CH_3COOH produced by several enzymes), and the other one producing the pH variation through a cascade of ET reactions using at the end a pH-dependent electron acceptor (modification of gate electrode), as recently reported in many papers operating EnFETs in the extended base configuration, later discussed in the present review.

2 | ENZYME-BASED FETs

EnFETs are defined as bioelectronic devices based on the coupling of an enzyme layer and an ISFET.^[18,20] The ISFET was developed by Bergveld in 1970 as the first miniaturized silicon-based chemical sensor.^[21] Figure 2a reports the scheme of an ISFET that consists of three terminals, notably source, drain, and gate. The device comprises a *p*-doped semiconductor body, source and drain heavily *n*-doped, an intermediate region modified with a dielectric layer (e.g., SiO_2 obtained through thermal oxidation of silicon), and a gate surface that is covered with an insulator layer (e.g., silicon nitride Si_3N_4 , tantalum pentoxide Ta_2O_5 , etc.),^[22,23] being sensitive to hydrolysis reaction (interactions with H^+ available in the solution). To operate an ISFET, the gate voltage (V_G) applied, is kept constant with respect to a reference electrode (e.g., $Ag/AgCl$ or saturated calomel electrode).^[19] At a small positive biasing potential (V_G applied vs. source electrode that is grounded), the energy bands are bent downward, thus the majority carriers (holes) are depleted (phenomenon observed through the recombination with electrons (minority carriers)) without observing a net current passing between source and drain (within the electronic channel). However, at larger biasing potential the energy bands bend downward even more so that the intrinsic Fermi level (E_i) crosses over the Fermi level of *p*-doped semiconductor (E_F), which induces excess negative carriers (electrons) at the SiO_2 -Si interface (minority carriers' concentration > majority carriers concentration) leading to the formation of an inversion layer (or *n*-channel). Hence, the number of electrons present in the electronic channel can be controlled by tuning V_G . It is possible to define as the threshold voltage (V_T), the minimum value of V_{GS} that leads to the formation of the inversion layer.^[24,25]

Based on the magnitude of the biasing voltage, the ISFET can be operated in three different regions: (i) cut-

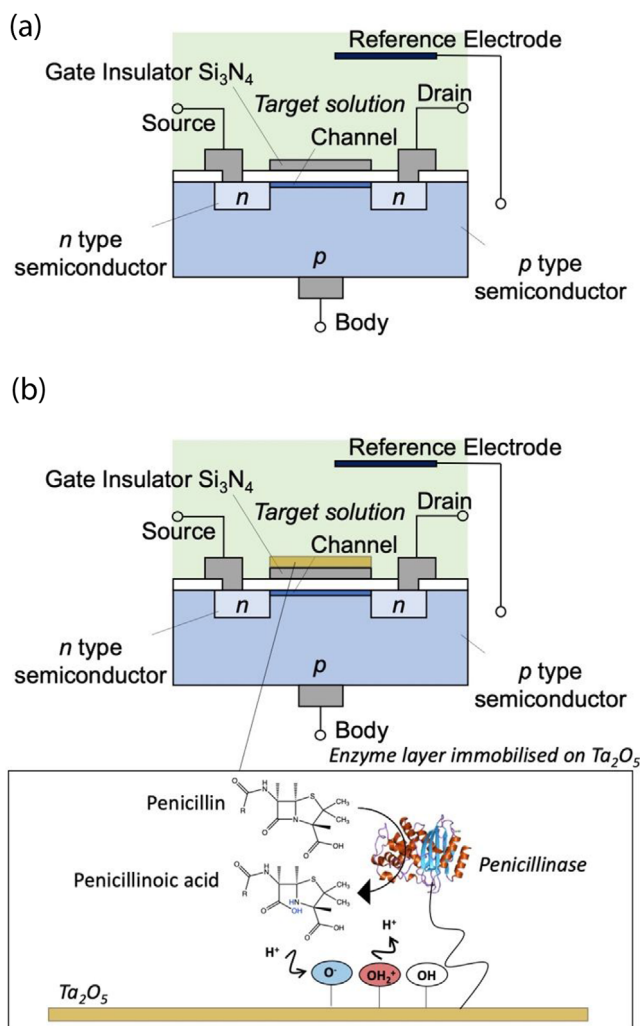


FIGURE 2 (a) Schematic representation of an ion-selective field-effect transistor (ISFET) and (b) Structure and working principle of a penicillin-sensitive enzyme-based field-effect transistor (EnFET) considering the enzymatic reaction (inset) and the site-binding model (inset)

off region, (ii) linear region, and (iii) saturation region. An ISFET operates in the cut-off region when $V_G < V_T$, hence the net current passing between source and drain is negligible. While applying a biasing voltage as $V_D << V_G - V_T$, the channel is formed and it electrically connects the source and drains, and I_{DS} is linearly dependent on source-drain voltage (V_{DS}) defining the ohmic region within the characteristic curve. The current of ISFET at saturation region is dictated by $V_D \geq V_G - V_T$, where the channel closed to the drain is pinched-off eventually leading to the I_{DS} saturation. The I_{DS} in linear and saturation regions can be defined by the following equations, respectively:

$$I_D^{lin} = \frac{W\mu C_i}{L} \left[(V_G - V_T)V_D - \frac{V_D^2}{2} \right] \rightarrow \text{with } V_D < V_D^{sat} \quad (1)$$

$$I_D^{sat} = \frac{W\mu C_i}{2L} (V_G - V_T)^2 \rightarrow \text{with } V_D > V_D^{sat} \quad (2)$$

where μ is the mobility, V_T is the threshold voltage, C_i is the capacitance of the gate insulator, V_G is the gate voltage, V_{DS} is source-drain voltage, $V_D^{sat} = V_G - V_T$, W is the channel width and L is the channel length of ISFET.^[27–29] In both equations, V_T is affected by the potential drops occurring at the additional interfaces:

$$V_T = E_{ref} - \psi_0 + \chi_{sol} - \frac{\phi_{Si}}{q} - \frac{Q_i + Q_{ss} + Q_B}{C_i} + 2\phi_f \quad (3)$$

where E_{ref} is the potential of the reference electrode, ψ_0 is the potential at the electrolyte/oxide interface, χ_{sol} is the surface dipole potential of the solution, ϕ_{Si} is the silicon work function, Q_i , Q_{ss} e Q_B are the charges located in the insulator, in the surface and interface states, and in the depletion region, respectively, and ϕ_f is the potential difference between the Fermi level of doped and intrinsic silicon. By considering an ISFET sensitive to H^+ , ψ_0 can be calculated according to the site-binding theory.^[30] This model assumes that the OH- groups exposed on the surface of the insulating layer are behaving as ionizable groups undergoing the H^+ dynamic exchange process (protonation/deprotonation), affecting the pH of the surrounding electrolyte. Hence, the dependence of ψ_0 with respect to pH can be expressed as follows:

$$\psi_0 = 2.303 \frac{kT}{q} \left(\frac{\beta}{\beta + 1} \right) (pH_{pze} - pH) \quad (4)$$

where pH_{pze} (point-of-zero charge) is the pH value for which $\psi_0 = 0$; k is the Boltzmann constant; T is the absolute temperature; β is a parameter which reflects the chemical sensitivity of the gate insulator and is dependent on the density of surface hydroxyl groups and the surface reactivity.^[26,28,31]

Afterward, ISFETs have been coupled with enzyme-modified membranes, as schematically shown in Figure 2b. EnFETs have been widely reported in the literature as ISFETs based biosensors where the H^+ gradient or pH change occurring nearby gate electrode is generated by specific enzymes in the presence of their substrates (pH gradient is proportional to substrate concentration). These devices have been developed for the detection of many clinically relevant metabolites like glucose, urea, creatinine, penicillin, and so forth.^[32–34]

Danielsson et al. reported in 1979 the development of an ‘enzyme transistor’ based on a palladium-coated semiconductor FET (Pd-MOSFET) for the detection of urea through its hydrolysis to NH_3 and CO_2 catalyzed by urease, where NH_3 is then protonated to NH_4^+ leading to an H^+ concentration change.^[35] The latter is detected through

the Pd-MOSFET exhibiting a non-linear dependence on NH_3 concentration in the range of 1–10 mM.

One year later, Caras and Janata realized an EnFET by exploiting a pH ISFET (sensitive to H^+ ions) where a membrane modified with penicillinase (converting penicillin to penicillinoic acid) was deposited on the gate insulating layer.^[15] The EnFET probe consists of the two separate ISFETs described above, one gate modified with a cross-linked albumin-penicillinase membrane (penicillin-sensitive gate), while the other gate has only a cross-linked albumin membrane and exhibits only pH response (reference gate), as reported in Figure 3. The device operating in differential mode exhibited a linear range up to 25 mM in pH 7.2 phosphate buffer (Figure 3). Although the penicillin EnFET showed analytical performance similar to the enzyme-modified macroelectrodes, the presented platform exhibited a longer lifetime, shorter response time, and smaller size (important during the scaling-up of the device production). Furthermore, Poghossian et al. reported a penicillin EnFET by using an H^+ ions sensitive Ta_2O_5 electrode modified with penicillinase, labeled as PenFET.^[37] The biosensor chip consisted of a dual system ISFET/PenFET in order to perform a differential measurement of voltage over pH variation, reporting a sensitivity of 120 ± 10 mV/mM in the concentration range of 0.05–1 mM penicillin G, a low detection limit of 5 μ M, a small hysteresis of less than 4 mV and a long lifetime (>1 year).^[38]

After Caras and Janata, Shul’ga et al. reported on the development of a GOx modified pH-sensitive EnFET aiming at extending the biosensor dynamic range.^[39] In this regard, the authors considered the reaction mechanism of GOx, as follows:^[40–42] (i) β -D-glucose + flavin adenine dinucleotide (FAD, oxidised form) \rightarrow D-glucono- δ -lactone + $FADH_2$ (reduced form); (ii) $FADH_2$ (reduced form) + $O_2 \rightarrow$ FAD (oxidised form) + H_2O_2 ; (iii) D-glucono- δ -lactone + $H_2O \rightarrow$ D-gluconate + H^+ (gluconic acid $pK_a \sim 3.8$), which in turn generates only one proton per oxidised glucose molecule, hence limiting the sensitivity of the EnFET biosensors. Moreover, the hydrolysis rate of D-glucono- δ -lactone depends on the working pH (e.g., at pH 8.0 it has a half-life of ~ 10 min, which decreases at lower pH). Thus, the presence of the slow rate-determining process, namely D-glucono- δ -lactone hydrolysis, affects the response time of the EnFET imposing several limitations on the thickness and morphology of a layer of immobilized GOx. In the air, considering O_2 as the final electron acceptor, the modified EnFET exhibited a dynamic linear range up to 1–1.5 mM probably due to the slow rate of enzymatic reaction (limited by low O_2 concentration). To extend the EnFET dynamic range, the final electron acceptor (i.e., O_2) has been replaced with $Fe(CN)_6^{3-}$ leading to the generation of three protons per oxidized glucose molecule. This easily occurs at $Fe(CN)_6^{3-}$ concentration \gg oxygen

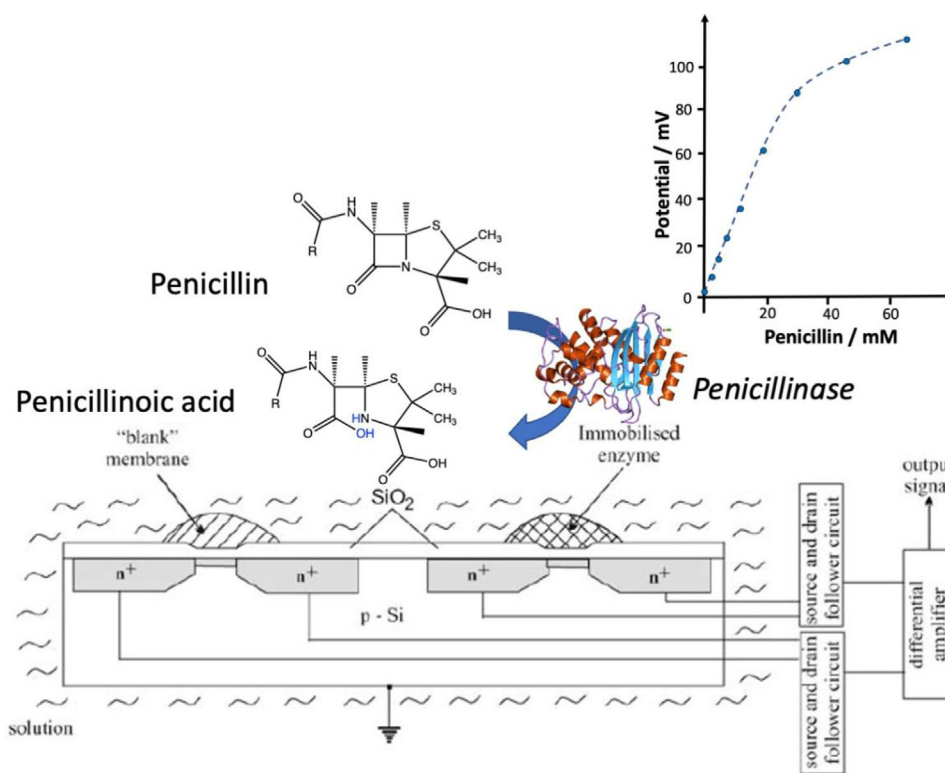


FIGURE 3 Schematic representation of a penicillinase modified enzyme-based field-effect transistor (EnFET) with a dual gate for differential measurements and the corresponding calibration curve with a dynamic linear range up to 25 mM in phosphate buffer pH 7.2. The scheme of the dual gate EnFET was adopted^[36] with permission of Springer-Nature

dissolved in the solution, while at a low concentration of $\text{Fe}(\text{CN})_6^{3-}$, there is competition between the electron acceptors leading to an S-shaped calibration curve, where it is possible to isolate the contribution of several physicochemical processes to the EnFET output, that is, (I) dissolved $\text{O}_2 > \text{Fe}(\text{CN})_6^{3-}$ concentration, (II) $\text{Fe}(\text{CN})_6^{3-}$ concentration \gg dissolved O_2 , (III) decrease of solutions buffer capacity, and (IV) pH-dependent enzyme kinetics, as shown in Figure 4.^[43]

Another urease-based EnFET was developed by Pijanowska and Torbicz by immobilizing the enzyme on a hydrated Si_3N_4 by using glutaraldehyde.^[44] The modified EnFET exhibited a linear range up to 20 mM, but as in all EnFETs, the output signal does not depend directly on the concentration of the enzymatic product. The output signal mainly depends on the concentration of H^+ in acid-base equilibrium with both the enzymatic product (i.e., NH_3) and the working buffer (i.e., phosphate buffer). However, the analytical performance of the developed urea-biosensor with direct immobilization of urease onto the silicon nitride surface is satisfactory for clinical applications, being in good correlation with spectrophotometric data recorded for the same samples.

After the initial investigations on the working principle of EnFETs, many scientists devoted their

attention to the immobilization strategies that could affect the enzyme loading/electronic communication and potentially increase the sensitivity of the device. In this regard, Kharitonov et al. developed an integrated NAD^+ -dependent EnFET for the detection of lactate.^[45] The surface of a SiO_2 gate was silanized with 3-aminopropyltriethoxysilane that was reacted with pyrroloquinoline quinone (PQQ) through 1-[3-(dimethylamino)propyl]-3-ethylcarbodiimide hydrochloride (EDC) coupling.^[46] After rinsing, the electrode surface was modified with amino- NAD^+ that was used to immobilize lactate dehydrogenase (LDH) by affinity interaction, as shown in Figure 5.

Hence, lactate could be oxidized to pyruvate with the contemporary reduction of NAD^+ to NADH , later re-oxidized by PQQ that was acting as a catalyst at the electrode surface. This reaction resulted in the production of a local pH gradient at the interface electrolyte/electrode promptly re-equilibrated by the bulk solution. However, PQQ plays a key role in the system because its continuous re-oxidation operated through the reduction of O_2 to H_2O_2 enabled two processes: (i) the recycling of PQQ generating a steady-state concentration of PQQ/PQQH₂ at the gate. Since all the species involved in the aforementioned redox processes are pH-dependent, the recycling allows

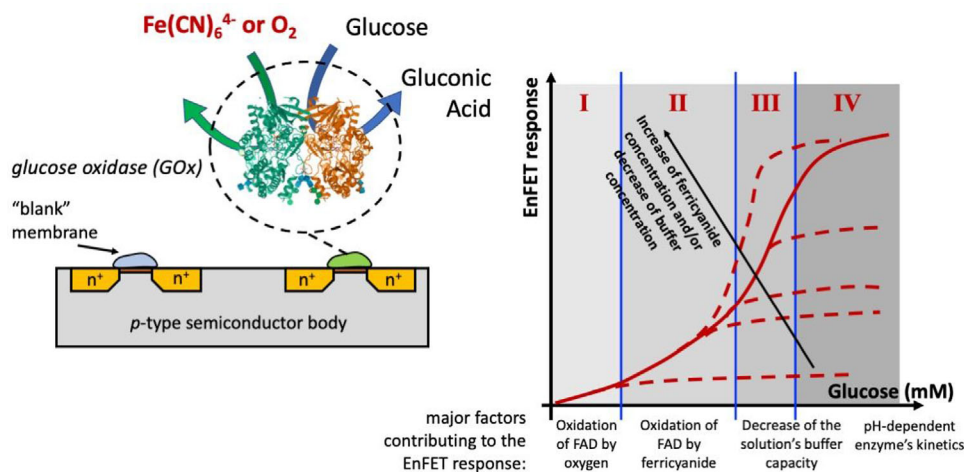


FIGURE 4 Schematic representation of a dual ion-selective field-effect transistor (ISFET) modified with glucose oxidase from *Aspergillus niger* (glucose enzyme-based field-effect transistor [EnFET]); General appearance of the calibration curve (solid line) of the glucose EnFET in the test solutions containing a one-base buffer and potassium ferricyanide under aerobic conditions. The biosensor response at different parts of the curve is controlled by different physicochemical processes occurring in the enzymatic layer as is indicated in the figure. Some tips about the modification of the curved shape when the concentrations of ferricyanide and/or buffer vary are given by a set of curves (shown by dashed lines) corresponding to different measurement conditions (see also the text). The graph reported in Figure 4 is adopted^[39] with permission of the American Chemical Society (ACS)

to keep constant the gate potential; and (ii) the presence of a constant pH gradient within the membrane that is proportional to the NADH generated through lactate oxidation catalyzed by LDH (injecting different concentration of lactate). The modified EnFET allowed the detection of lactate at 0.1 mM as the limit of detection (LOD)^[47] with a short response time (15 s). This work represents the first example of tailoring the working principle of a gate electrode through such a complex operation considering not only the H⁺ concentration variation created by the enzyme, that could be easily re-equilibrated by the bulk solution decreasing the sensitivity but considering the transport of H⁺ ions till the electrode surface through a cooperating effect of several catalysts. This certainly contributes to enhancing the sensitivity of the PQQ/NAD⁺-LDH modified EnFET. The same authors reiterated the system with another enzyme, notably nicotinamide adenine dinucleotide phosphate (NADP⁺)-dependent alcohol dehydrogenase (ADH) with similar performance. However, both devices were calibrated with different concentrations of NAD⁺ and NADP⁺ (keeping constant the enzyme-substrate concentration for both LDH and ADH).^[48] In this work, the authors aimed at monitoring the hydrolysis of NAD⁺ catalyzed by NAD oxidase or cholera toxin (subunit A). The proposed device could potentially be exploited to monitor many biological processes that imply NAD⁺ hydrolysis. At the same time, the research on EnFET based devices was addressed toward the detection of toxic compounds like pesticides that are also acting as inhibitors of many enzymes catalyzing H⁺ dependent reactions.^[49]

It should be underlined that in these devices the analytical parameters like dynamic range and operational/storage stability are strongly dependent on the inhibition mechanism, notably reversible, irreversible, or competitive.^[50] Indeed, the detection of organophosphorus and carbamate compounds is enabled by their ability to inhibit cholinesterases (ChEs) through their interaction with the serine OH- group in the enzyme active site.^[51] The decrease in ChEs activity after its interaction with pesticides can be effectively monitored through the EnFET based biosensors, allowing the toxicity assessment of organophosphorus and carbamate pesticides.^[52] Considering several devices reported in the literature, ChEs based devices exhibited a LOD as low as 30 pM for diisopropyl fluorophosphate, 0.5 μM for paraoxon-ethyl, 5 μM for paraoxon-methyl, and 0.2 μM for trichlorfon.^[36] Due to their capability of being easily integrated into biosensor arrays, inhibition-based EnFETs based on different enzymes jointly with multivariate analysis could potentially be exploited as an environmental toxicity screening device.

However, it should be considered the fact that an array of EnFETs implies the needing for several transistors with different active layers (different enzymes for several substrates) compiled in one device that would hinder the possibility of miniaturizing the biosensor array.^[53] Conversely, Van der Spiegel and his co-workers, in 1983, proposed a multi-species microprobe for potentiometric detection by using chemically sensitive membranes. In particular, the authors created an extension of the gate

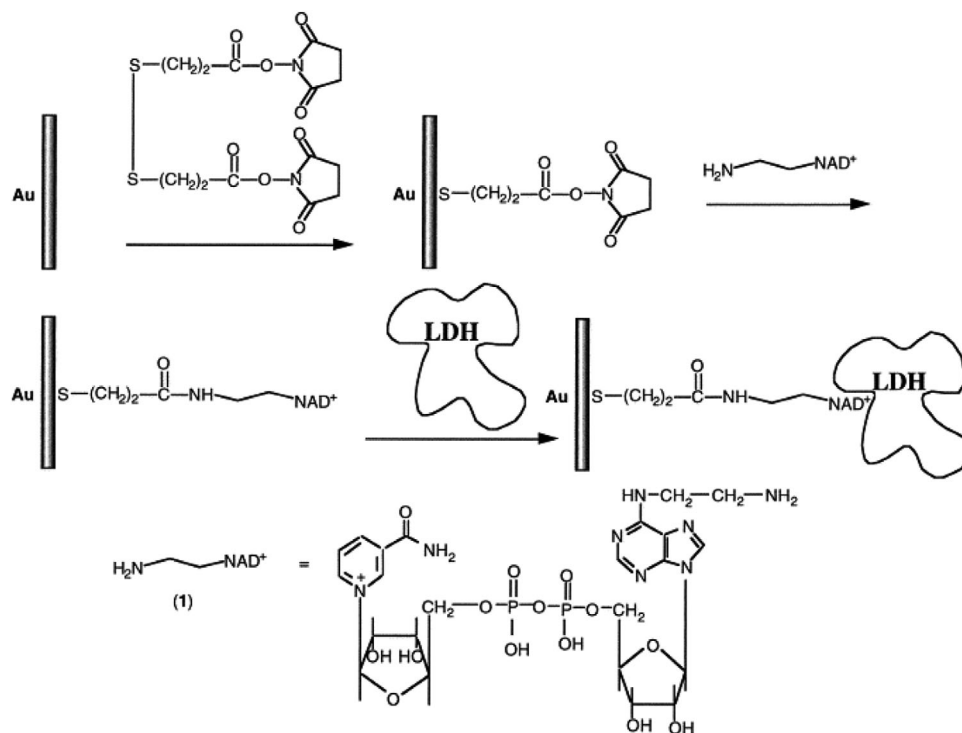


FIGURE 5 Stepwise organization of the nicotinamide dinucleotide (NAD^+)-monolayer-modified Au-electrode and affinity binding of an NAD^+ -dependent enzyme to the electrode. The content is reproduced^[45] with permission of Elsevier Ltd

within the transistor that was connected through a coaxial line to other electrodes (extended gate) modified with several inorganic layers sensitive to different species like iridium oxide (IrO_2) sensitive to H^+ , silver chloride (AgCl) sensitive to Cl^- and lanthanum fluoride (LaF_3) sensitive to F^- .^[54] This was the first report about a multi-species potentiometric sensor based on planar silicon fabrication through effective patterning of the active layer that allowed to obtain a miniaturized device, named EG-FET.

3 | ENZYME-BASED EG-FETs

EG-FETs comprise two components, namely a conventional ion-sensitive electrode and a MOSFET, as schematically reported in Figure 6a,b.^[55,56] In particular, the ion sensing electrode is connected with the gate of the MOSFET that is not anymore exposed to the electrolyte solution as a key step toward device miniaturization. In addition to miniaturization and the possibility of on-chip integration in multisensor arrays for parallel sensing, the main advantage is the easiness of sensing electrode exchange because the FET is kept outside of the usually wet analyte environment.^[57,58] For an EG-FET, V_T needs to consider the interface potentials generated by the reference electrode and the sensing electrode, which can

be summarized as follows:

$$V_T(\text{EGFET}) = \Delta V_{ref} + V_T(\text{MOSFET}) \quad (5)$$

where ΔV_{ref} is the voltage measured at the ion sensing interface with respect to the reference electrode and $V_T(\text{MOSFET})$ is the threshold voltage of the MOSFET connected.

Similar to ISFETs, EG-FETs have been exploited for chemical ion sensing, with particular emphasis on the detection of H^+ ions, hence pH variations.^[60] To this extent, many nanomaterials, both carbon-based nanomaterials (e.g., multiwalled carbon nanotubes,^[61–63] reduced graphene, etc.) and metal/metal oxide-based nanoparticles^[64–66] have been used to develop external gate electrodes that exhibited a pH sensitivity by means of potentiometric measurements.^[67–69] In this regard, Yin et al. reported on the development of an H^+ ion-sensitive EG-FET by using an indium tin oxide (ITO) electrode modified with tin oxide (SnO_2) by a sputtering method.^[70] The device exhibited a shift in the V_T with respect to pH change with a sensitivity of approximately 58 mV/pH (within the H^+ concentration range 10^{-2} – 10^{-12} M). However, the authors succeeded to demonstrate the possibility of decreasing the voltage drift by modifying ITO electrodes (110 mV of voltage drift over 18 h) with SnO_2 , which showed only 9.1 mV of voltage drift over the same time

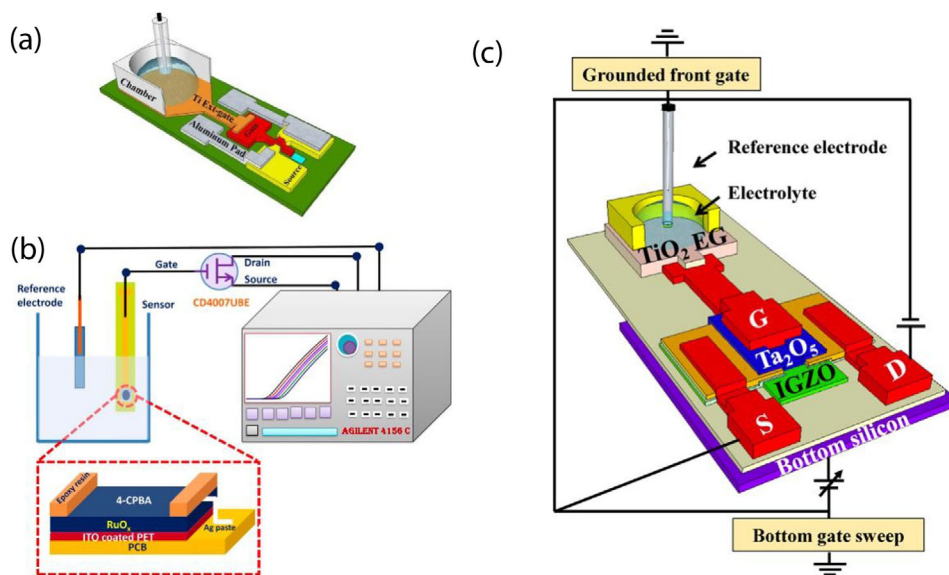


FIGURE 6 (a) Schematic representation of an extended-gate field-effect transistor (EG-FET), (b) Schematic illustration of the RuOx on PET-based EG-FET sensor and EG-FET measurement unit, and (c) Schematic representation of the α -IGZO based dual-gate (DG) EG-FETs and description of the DG operation mode. Part (a) reproduced^[56] with permission of the American Institute of Physics (AIP). Parts (b) and (c) are reproduced^[58,59], respectively, with permission of Elsevier Ltd

probably because the additional layer hinders the possibility of surface passivation leading to higher stability of the modified electrode. In the same year, Chi et al. demonstrated as the performance of an EG-FET based on the same modification is not affected by ambient light.^[71] Besides ITO electrodes modified with SnO₂, also titanium nitride (TiN) has been exploited as H⁺ ion-sensitive layer, exhibiting a sensitivity of 57 mV/pH.^[72] Furthermore, Batista and Mulato reported a sol-gel method used to produce a zinc oxide (ZnO) film that was used in an EG-FET to detect pH variations. The ZnO film was investigated as a pH sensor in the range of 2–12, exhibiting a sensitivity of 38 mV/pH.^[73] Such low sensitivity might have arisen from the contamination by other organic compounds (during synthetic steps) that limited the number of surface sites available for H⁺ “binding”.

Recently, Jang and co-workers demonstrated the possibility to increase the sensitivity of pH-sensitive EG-FET by using silicon-on-insulator (SOI) technology.^[59] Differently, from a conventional MOSFET, SOI technology consists of a layered system silicon-insulator (metal oxide)-silicon instead of a conventional *p*-doped silicon substrate. Then, the buried oxide layer (insulator) is made of a ternary oxide, namely amorphous InGaZnO (In₂O₃:Ga₂O₃:ZnO, the composition ratio of target = 1:1:1 mol%, α -IGZO), was topped by an additional silicon layer.^[74] Next, a Ta₂O₅ gate dielectric layer was deposited onto the gold pad contacts for source and drain, respectively. After that, a 150-nm-thick aluminum for the front gate electrode and 30-nm-thick titanium oxide (TiO₂) film was deposited as a pH-

sensitive layer on top of the titanium extended gate. The schematic representation for the dual-gate (DG) operation of α -IGZO based TiO₂ EG-FET is reported in Figure 6c. Unlike the conventional single gate (SG) operation (the front reference electrode was biased), the bottom gate of DG was biased with the grounded front reference electrode. The authors succeeded to demonstrate that the α -IGZO based TiO₂ EG-FET exhibited sensitivity toward H⁺ ions detection of 129.1 mV/pH which is beyond the “Nernst limit” (59 mV/pH) due to the capacitive coupling between the front and bottom gate oxides, also showing remarkable stability over time.

Besides H⁺ ions sensing, EG-FETs based both on non-enzymatic and enzymatic reactions generating a pH change were successfully used to test several metabolites like urea, glucose, and so forth.^[55,75,76] For example, Chen and co-workers developed an EG-FET for the detection of urea-based on urease deposition onto SnO₂ modified ITO electrode as an extended sensing electrode.^[77] The enzyme was immobilized by physical entrapment in a photo-polymerized membrane of poly(vinyl alcohol), *N*-methyl-4-(4'-formylstyryl)pyridinium methosulfate acetal achieving a dynamic range from 0.31 to 120 mg/dl in 5 mM phosphate buffer solution and a response time of about 2 min. In a similar approach, several enzymes based EG-FETs have been proposed for the detection of glucose by exploiting GOx, whose reaction product (gluconic acid) is undergoing hydrolysis reaction.^[78] For instance, Wang et al. reported an EG-FET based on an aluminum-zinc-oxide (AZO) nanostructured sensing

electrode that showed promising sensing characteristics such as a sensitivity of $60.5 \text{ A mM}^{-1} \text{ cm}^{-2}$ up to 13.9 mM (upper limit of the dynamic linear range) for a disposable biosensor.^[79] The morphology of AZO nanostructures is related to aluminum content. Well-matched ratios of aluminum and ZnO showed higher crystallinity and better conductivity, resulting in superior sensing characteristics.

EG-FETs have been proposed as multipurpose sensing platforms by simply replacing the sensing electrode.^[80] However, this is not easy to realize with enzymes. In particular, Lin et al. integrated an EG-FET into a microfluidic chip to significantly reduce the volume of samples to be tested.^[75] An Al_2O_3 sensing membrane with a thickness of 50–80 nm was tested toward pH variations in the range of 6–8 showing a sensitivity of 37.45 mV/mM . To exploit the same device for multiple detection processes, the authors immobilized the enzymes, namely GOx and urease with magnetic nanoparticles within an alginate Ca^{2+} cross-linked microcube. After injecting the microcubes in the microfluidic chip, they were driven through the application of an external magnetic field in correspondence of the gate electrode where both enzymes were producing an in-situ pH change detected by Al_2O_3 modified electrode. Alternatively, the same platform was used to detect the bladder cancer-related protein apolipoprotein A1 (APOA1) by using freely diffusing magnetic nanoparticles instead of being embedded in the hydrogel. Since APOA1 carries a small charge that cannot be directly detected, thus the capturing antibody was conjugated with magnetic nanoparticles, forming afterwards a sandwich with the detecting antibody conjugated with a DNA strand used as charges amplifier as shown in Figure 7a,b.

After sandwich formation with different APOA1 concentrations (0.33–33 nM as an explored range), an external magnetic field was applied to attract the complex to the gate electrode detecting a variation of charges at the interface electrode solution inducing a gate voltage change. As further proof of the APOA1 detection mechanism, the authors explored different base-pair (bp) lengths showing a sensitivity enhancement (approximately 3-fold) between 20 and 90 bp lengths. With a similar approach, Kamahori and co-workers reported the development of an EG-FET based on enzyme-linked immunosorbent assays (ELISA) where the detecting antibody is conjugated with acetylcholinesterase (AChE), that produced a pH variation nearby the electrode surface.^[81] The proposed ELISA-based EG-FET sensor was able to detect Interleukin 1 at concentrations as low as 1 fM .

Similar to ISFETs, also EG-FETs have been used to develop inhibition-based biosensors. In this regard, Sasipongpana et al. reported an EG-FET for the detection of carbaryl pesticide through the inhibition of

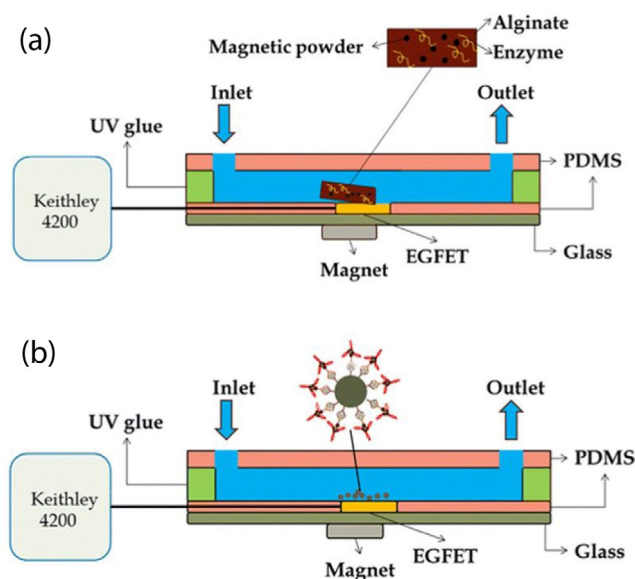


FIGURE 7 (a) Enzyme immobilization and sensing processes. Magnetic enzyme-embedded alginate microcubes were injected into the flow channel and adsorbed on the extended-gate field-effect transistor (EG-FET) surface by an external magnetic field. After the solution to be tested was injected for the reaction, the electrical signal was measured. (b) Process for protein measurement using the immunomagnetic beads analysis method. After the immunomagnetic beads were injected into the inflow channel and adsorbed onto the EG-FET surface by an external magnetic field, the electrical signal was measured. Parts (a) and (b) are adapted^[75] with permission of Springer-Nature

AChE, which hydrolyses acetylcholine to acetate and choline, then the acetate ions are undergoing protonation/deprotonation equilibrium.^[82] The last reaction step enabled the monitoring of potential changes over pH variation by using an ITO sensing electrode with a sensitivity of about 45.27 mV/pH which is close to the commercial ISFET (about 50 mV/pH). Carbaryl pesticides are reported to inhibit AChE reaction by carbamylated the enzyme, namely interacting with a serine residue available in the esteratic site. The proposed ITO-EG-FET was able to detect carbaryl in the concentration range of $0.001\text{--}1 \text{ mM}$. Many other examples of EG-FETs based on the enzymatic inhibition by pesticides have been reported in the literature with similar detection mechanisms and analytical figures of merit (i.e., sensitivity, LOD dynamic linear range, selectivity, etc.).

As a further step toward sensing integration and process scaling up, the production of enzyme-based EG-FETs has been rerouted toward flexible materials in order to be used as wearable biosensors for metabolites continuous detection, bearing in mind that the sensing electrode is still electrically wired with the transistor and the transistor is not exposed to the tested sample.

4 | ENZYME BASED EG-OFETs

During the last three decades, the improved physical understanding of transport and structure-property relationships about π -conjugated organic semiconductors (OSCs) has certainly contributed to the exponential development of OFETs (also known as OFETs).^[83–85] Besides OFETs, OSCs have been reported for several applications like organic solar cells and light-emitting devices.^[86] The field-effect mobility (μ), which is the main materials-related figure of merit of an OFET, has increased from low values $< 10^{-3} \text{ cm}^2 \text{ V}^{-1} \text{ s}^{-1}$ more than 30 years ago to values $> 1\text{--}10 \text{ cm}^2 \text{ V}^{-1} \text{ s}^{-1}$ that are now exceeding those of benchmark thin-film amorphous silicon devices ($0.5\text{--}1 \text{ cm}^2 \text{ V}^{-1} \text{ s}^{-1}$).^[87–89] OFETs based biosensors have been largely reviewed in the last 10 years considering different possible applications for the detection in clinical analysis (nucleic acids, metabolites, proteins, pathogens, human cells, and drugs).^[63,90,91] In parallel with enzyme-based OFETs, the OFETs based on antigenic interaction or DNA/DNA base pair matching as biorecognition events have been widely explored for the detection of many clinically relevant biomarkers.^[92,93] Indeed, one of the key achievements in the field is certainly the possibility to perform label-free detection at the single-molecule level by using a millimeter size electrolyte gated OFET, as reported for the first time in 2018.^[94] The sensing mechanism behind such a high sensitivity was explained considering that each antibody bears a dipole moment oriented from Fc to Fab region that is re-oriented in the presence of an applied electric field by means of electrostatic interaction. Next, the interaction antigen/antibody (biorecognition event) triggers a conformational rearrangement in the Fab region that is transferred to the Fc region creating several defects in the oriented dipoles' layer.^[95] After the first attempt, electrolyte-gated OFETs have been reported for several applications based on antigen/antibody interactions.^[93,96–99] Beyond immunometric or genomic electrolyte gated OFETs, also OECTs have been operated as potentiometric sensors exhibiting very high LODs. Indeed, many OECTs reported in the literature based on immunometric reactions exhibit a LOD in the attomolar range or lower.^[91,100–102]

Besides immunometric or genomic biosensors based on electrolyte gated OFETs and OECTs, enzymes have been merged both with OECTs and OFETs by developing the extended-gate OFETs (EG-OFETs).^[103,104] In particular, the research on enzyme-based OECTs has been pioneered by Malliaras as resulting from the literature.^[103,105,106] On the other hand, the research on enzyme-modified EG-OFETs has been pursued mainly by Minami's research group to the best of our knowledge.^[104,107,108]

In 2004, Malliaras and co-workers demonstrated a simple transistor based on a commercially available conducting polymer poly(3,4-ethylenedioxythiophene) doped with poly(styrenesulfonate) (PEDOT:PSS), capable of sensing glucose in a neutral pH buffer solution.^[109] The mechanism involves the sensing of hydrogen peroxide. Afterward, Malliaras and co-workers reported on the development of an enzyme-based OECT biosensor for the detection of glucose through its oxidation catalyzed by GOx floating in the electrolyte solution, where O_2 acts as the final electron acceptor generating H_2O_2 further decomposed at a Pt-gate electrode. The latter was combined with a PEDOT:PSS OECT showing a logarithmic dependence of the offset voltage on glucose concentration up to 1 mM.^[103] In another work, the same authors adopted ADH as a NAD-dependent enzyme to develop a breathalyzer for the detection of blood alcohol content (BAC). In this fashion, the OECT-breathalyzer easily detects ethanol in the breath equivalent to BAC from 0.01% to 0.2%.^[105] Other enzyme-based OECTs have been reported by other research groups.^[106,110,111]

For enzyme-based EG-OFETs, Minami and his co-workers reported on the development of a biosensor for lactate detection in aqueous media.^[112]

The OFET was fabricated by depositing the aluminum gate onto a glass slide, afterward covered by a dielectric layer of aluminum oxide (Al_2O_3) and a tetradecylphosphonic acid self-assembled monolayer (SAM). Next, the gold pads as S and D electrodes were evaporated, followed by the deposition of poly(2,5-bis(3-hexadecylthiophene-2-yl)thieno[3,2-b]thiophene) (PBTTT-C16) as OSC. The aluminum gate electrode was connected to the extended gate, notably, a gold electrode (deposited on polyethylene naphthalate [PEN] flexible substrate) modified with an osmium-redox polymer (ORP) able to reduce Os^{3+} to Os^{2+} shuttling the electron to the heme site of the horseradish peroxidase (HRP), which is converting H_2O_2 generated by the main redox reaction, namely the oxidation of lactate catalyzed by lactate oxidase (LOx), as shown in Figure 8a. The device exhibited both high selectivity (other potential interferents like glucose, urea, and so forth, showed an output response of 5%–10% of lactate signal) and sensitivity (Figure 8b,c). The interferences from urea and glucose might be related to the local pH gradient affecting the V_T , hence the output signal. Moreover, CaCl_2 , MgCl_2 , and NaCl might cause some voltage drift due to the ionic strength while *p*-cresol can potentially compete with ORP for the electrons shuttling toward HRP. However, the LOD and the limit of quantification were estimated to be 66 and 220 nM, respectively. Later, this type of extended gate was employed with another OFET component where the authors replaced the OSC previously used with dinaphtho[2,3-b:2',3'-f]thieno[3,2-b]thiophene and

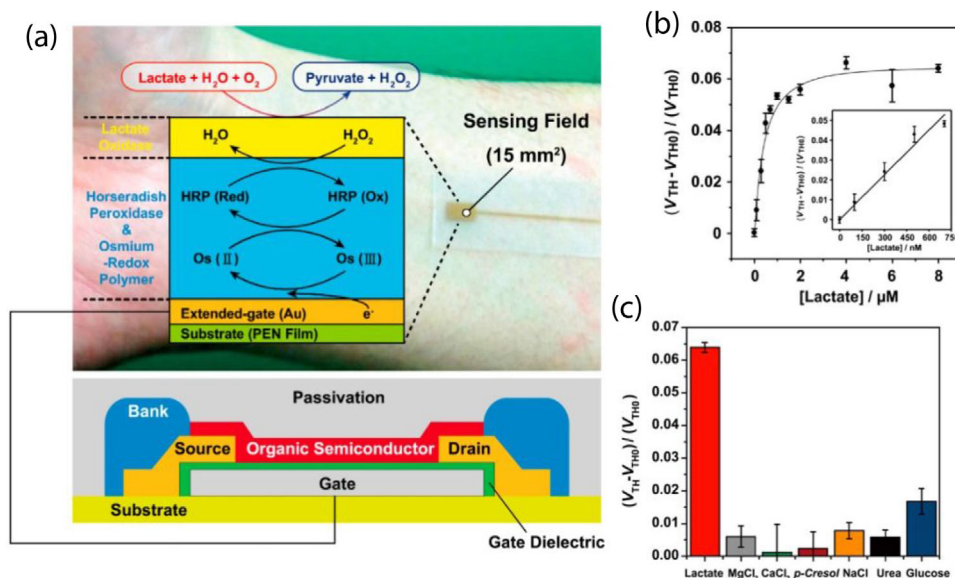


FIGURE 8 (a) Schematic representation of lactate oxidase modified extended gate-organic field-effect transistor (EG-OFET), (b) Changes in threshold voltage (V_T) of the OFET device by adding lactate at various concentrations in a HEPES-buffer solution (100 mM) at pH 7.4 at room temperature. The inset shows the lower end of the titration, (c) Changes in the threshold voltage (V_T) of the OFET device by the addition of various analytes (8 μM) in a HEPES buffer solution (100 mM) at pH 7.4 at room temperature. Parts (a–c) were reproduced^[112] with permission of Elsevier Ltd

the dielectric layer with a mixed layer of pentadecylfluorooctadecylphosphonic acid and Al_2O_3 .^[113,114] However, the proposed EG-OFET device did not show any substantial improvement in the analytical figures of merit.

In the same year, Minami et al. proposed a similar configuration for the OFET part except for the dielectric that this time consisted of Al_2O_3 and tetradecylphosphonic acid self-aligned monolayer able to decrease the operating voltage range (<3 V).^[115] Herein, the EG was modified with ORP, HRP to reduce hydrogen peroxide to H_2O , and diamine oxidase able to oxidize diamine compounds (i.e., histamine, putrescine, etc.), also known as biogenic amines, but not polyamines like cadaverine, spermidine, and so forth.^[116] Biogenic amines are produced by bacteria through the decarboxylation of amino acids or by the amination of aldehydes and ketones. Indeed, they are used as a biomarker in food sensing to estimate the freshness of certain foods like meat, vegetables, and fish.^[117,118]

In 2016, Minami et al. reported the first selective nitrate biosensor based on the same OFET configuration. The extended gate electrode was modified with a SAM of 2-aminoethanethiol, later modified with *N*-methyl-*N'*-(carboxyethyl)-4,4'-bipyridinium reacted with 1-hydroxybenzotriazole and EDC through a covalent bond. Finally, nitrate reductase from *Aspergillus niger* was drop-cast onto the modified electrode and cross-linked with glutaraldehyde.^[119] In particular, the bipyridinium moieties were exploited as ET mediators able to regenerate the initial redox state of the enzyme, while dithionite

is acting as an electron relay toward nitrate reduction. The LOD of nitrate in water was estimated to be 45 ppb, which is comparable with LOD reported for the conventional detection methods. However, the selectivity was also tested considering some representative small anions such as chloride (Cl^-), thiocyanate (SCN^-), hydrogen phosphate (HPO_4^{2-}), and bicarbonate (HCO_3^-) without any clear output response in the entire concentrations range investigated for nitrate ions.

Almost in parallel with the research work of Minami et al., Tokito and co-workers turned their interest toward the integration of EG-OFETs into printed organic circuits aiming at developing wearable biosensors.^[120] In this regard, conventional OFETs were replaced by organic thin-film transistors (OTFTs) to realize ultra-thin, lightweight, and flexible sensing devices with miniaturized electronic components. The device consisted of three terminals: source, drain and gate in silver, a blend solution of 2,7-dihexyl-dithieno[2,3-d;2',3'-d']benzo[1,2-b;4,5-b']dithiophene and polystyrene as OSC and a parylene dielectric layer, was printed on a PEN substrate, as shown in Figure 9a.^[121] The silver sensing surface was modified with a mixed layer of carbon and Prussian blue (PB), able to selectively reduce H_2O_2 at a smaller potential compared to other catalysts. To sense lactate, this active layer was modified with LOx physically entrapped by chitosan (Figure 9b,c).

The proposed device exhibited a very limited linear range (0.1–0.5 mM) as well as a sensitivity and LOD

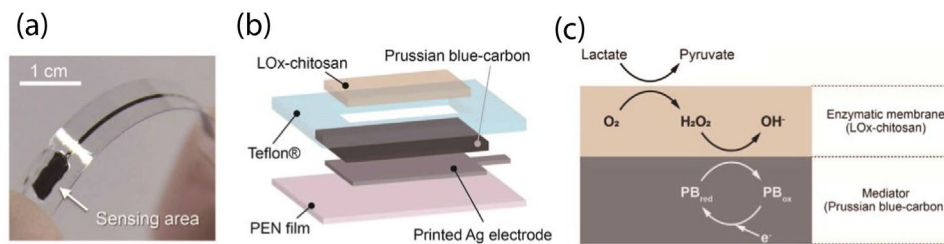


FIGURE 9 Structure and electrochemical characteristics of the lactate sensor: (a) Photograph of the fabricated lactate sensor electrode. The sensing area was 15 mm², (b) schematic diagram of the lactate sensor electrode, and (c) the principle of lactate sensing. Parts (a–c) were adapted^[121] with permission of Springer-Nature under a Creative Commons Attribution 4.0 International License, <http://creativecommons.org/licenses/by/4.0/>

comparable with other enzymatic amperometric biosensors. However, the main advantage of EG-OTFTs is related to the printability of the entire device without the needing for a potentiostat controlled measurement. A similar approach was proposed for the detection of β -D-glucose in externally secreted body fluids such as tears, saliva, and sweat. Later, the same authors proposed the detection of 1,5-anhydroglucitol (1,5-AG) and glucose, which are monosaccharides used as biomarkers of diabetes. An OFET-based biosensor combined with a PB electrode, modified with GOx or pyranose oxidase (POx), was utilized for the detection of the monosaccharides. Both electrodes could potentially be used simultaneously as an array because of the low cross-reactivity of the substrates on the neighboring electrode (i.e., for glucose the POx-PB modified electrode).^[122]

Besides some physical limitations like the small voltage shifts (with respect to V_T) observed during the redox processes, the needs of an Ag/AgCl reference electrode to fix the potential within the electrochemical cell, EG-OFETs and EG-OTFTs still hold some advantages regarding their potential integration to develop enzyme-based either wearable or array biosensors.^[123] (Tables 2–3)

5 | CONCLUSIONS AND FUTURE PERSPECTIVES

The enzyme-based transistors herein reviewed belonging different groups, namely EnFETs, enzyme-based EG-FETs, and enzyme-based EG-OFETs, own a few common features: (i) the gate electrode is modified with enzymes or connected with an extended gate (additional electrode) modified with enzymes for the analytical detection of the corresponding substrate (target analyte); (ii) the output signal, namely the drain-source current (I_{DS}), is related with the variation of the V_T . The latter depends on the concentration of ions such as H^+ involved in the redox equilibrium (EnFETs or enzyme-based EG-FETs) or on the vari-

ation of the equilibrium voltage induced by the ET from the active center of the enzyme to the electrode (and vice versa) through several electron relays (organic ET mediators); (iii) the lack of the amplification factor on the voltage change occurring at the gate terminal (or extended gate electrode), which improve neither the sensitivity (LOD still in the μ M range) nor the dynamic linear range (mostly due to Nernstian dependence of voltage on analyte concentration).^[124,125]

From a future perspective, we should acknowledge the need for bioelectrochemists (experts in microbial and enzymatic bioconversions) to be involved in such research topics especially considering the complex architectures of the extended gate electrodes. This would play a key role in distinguishing enzyme-modified electrodes based on the ET pathway, namely first, second and third generation. So far, the presented extended gates cannot be exclusively classified in any of the aforementioned groups. For instance, considering a recent report on LOx modified EG-OFET, we could consider such electrode in either of the three groups because LOx, as a flavin mononucleotide-dependent oxidoreductase, is an oxygen-sensitive enzyme, thus producing H_2O_2 as a reaction by-product. At this step, we could consider the electrode within the first generation group by monitoring O_2 consumption or H_2O_2 production with a potentiometric measurement with respect to a reference electrode. However, by adding HRP in the enzyme sequence to reduce H_2O_2 to H_2O , we should observe a DET that triggers the variation of the equilibrium potential based on the substrate concentration (monitored by potentiometric measurements). This architecture would follow within the third generation considering the DET process involving HRP. The DET approach has been adopted by Inal and co-workers through the immobilization of GOx onto n-type copolymer P-90 deposited both on the gate electrode and in the channel to develop an enzyme-based OECT for the detection of glucose in bodily fluids.^[126] Alternatively, the introduction of an ORP as an electrons relay would

TABLE 1 Main features of enzyme-based field-effect transistors (EnFETs) encompassing sensing enzyme, molecule inducing pH variation, dynamic linear range (mM), and limit of detection (mM). Not available data are reported as N/A

Sensing enzyme	Molecule inducing pH variation	Dynamic linear range (mM)	Limit of detection (LOD) (mM)	Ref.
Urease	NH ₃	< 1	N/A	[35]
Penicillinase	Penicillinoic Acid	0.1–25	N/A	[15]
Penicillinase	Penicillinoic Acid	0.05–1	5 × 10 ⁻³	[38]
Glucose oxidase	Gluconic Acid	< 1.5	N/A	[39]
Urease	NH ₃	< 20	N/A	[44]
Lactate dehydrogenase	Pyrroloquinoline Quinone	N/A	0.2	[48]
Alcohol dehydrogenase	Pyrroloquinoline Quinone	N/A	0.1	[48]
Acetylcholinesterase	CH ₃ COOH	0.03–500 (x 10 ⁻⁶) (diisopropyl fluorophosphate) 1–50 (x 10 ⁻³) (paraoxon ethyl) 5–50 (x 10 ⁻³) (paraoxon methyl) 0.2–100 (x 10 ⁻⁴) (trichlorofon)	0.03 × 10 ⁻⁶ (diisopropyl fluorophosphate) 0.5 × 10 ⁻⁴ (paraoxon ethyl) 5 × 10 ⁻³ (paraoxon methyl) 0.2 × 10 ⁻⁴ (trichlorofon)	[36]

The main features of EnFETs are summarised in Table 1.

TABLE 2 Main features of EG-FETs encompassing bioreceptor, pH-sensitive layer, dynamic linear range (mM), and sensitivity. Not available data are reported as N/A. Abbreviations: Acetylcholinesterase (AChE), aluminium-zinc-oxide (AZO), aluminium oxide (Al₂O₃), apolipoprotein A1 (APOA1), anti-interleukin-1/acetylcholinesterase (Anti-IL1/AChE), glucose oxidase (GOx), indium tin oxide (ITO), tin oxide (SnO₂)

Bioreceptor	pH-sensitive layer	Dynamic linear range (mM)	Sensitivity	Ref.
Urease	SnO ₂ -ITO	N/A	N/A	[77]
GOx	AZO	<13.9	60.5 μA/mM	[78]
GOx	Al ₂ O ₃	N/A	37.3 mV/mM	[75]
APOA1	Al ₂ O ₃	0.33–33 (x 10 ⁻⁶)	N/A	[75]
Anti-IL1/AChE	ITO	N/A	N/A	[81]
AChE	ITO	0.001–1	45.3 mV/pH	[82]

The main features of EG-FETs are summarised in Table 2.

TABLE 3 Main features of extended gate-organic field-effect transistors (EG-OFETs) encompassing extended gate platform, organic semiconductor, dynamic linear range (mM) and limit of detection (mM). Not available data are reported as N/A. Abbreviations: 1-hydroxybenzotriazole (HOBt), 2-aminoethanethiol (AE), 2,7-dihexyl-dithieno[2,3-d;2',3'-d']benzo[1,2-b;4,5-b']dithiophene (DTBDT-C6), diamine oxidase (DAOx), glucose oxidase (GOx), gold electrode (Au), horseradish peroxidase (HRP), lactate oxidase (LOx), nitrate reductase (NR), osmium redox polymer (ORP), poly{2,5-bis(3-hexadecylthiophene-2-yl)thieno[3,2-b]thiophene} (PBTTT), polystyrene (PS), Prussian blue (PB), pyranose oxidase (POx), tetradecylphosphonic acid (C₁₄-PA)

Extended-gate platform	Organic semiconductor	Dynamic linear range (mM)	Limit of detection (mM)	Ref.
LOx/HRP/ORP/Au	PBTTT-C16	<0.74	0.07	[112]
DAOx/HRP/ORP/Au	PBTTT-C16	<0.01	0.0012	[115]
NR/HOBt/AE/Au	PBTTT C14-PA	<0.004	0.0004	[119]
LOx/PB/carbon	DTBDT-C6-PS	0.1–0.5	N/A	[120]
GOx/PB/carbon	DTBDT-C6-PS	N/AN/A	N/AN/A	[122]
POx/PB/carbon				

The main features of EG-OFETs are summarised in Table 3.

include the modified surface within the second-generation group. This misunderstanding on conceiving the modified surface based on the ET pathway could be easily solved considering the literature on enzyme-based electrochemical biosensors toward the development of third-generation enzyme-based potentiometric biosensors (i.e., using PQQ-dependent glucose dehydrogenase, cellobiose dehydrogenase, fructose dehydrogenase, etc.)^[127,128] or chimeric redox enzymes (i.e., calmodulin modulated PQQ-dependent glucose dehydrogenase)^[129,130] that could be later integrated as an extended gate into an organic field-effect transistor. Although this would contribute to avoiding ineffective gate terminal modifications, it will not help to improve the analytical figures of merit (i.e., sensitivity, LOD, dynamic linear range, etc.) of such biosensors.

ACKNOWLEDGMENTS

Lucia Sarcina and Eleonora Macchia contributed equally to this work. The following funding agencies are acknowledged: Academy of Finland projects #316881, #316883 “Spatiotemporal control of Cell Functions”, #332106 “ProSiT—Protein Detection at the Single-Molecule Limit with a Self-powered Organic Transistor for HIV early diagnosis”; Biosensori analitici usa-e getta a base di transistori organici auto-alimentati per la rivelazione di biomarcatori proteomici alla singola molecola per la diagnostica decentrata dell’HIV (6CDD3786); Research for Innovation REFIN—Regione Puglia POR PUGLIA FESR-FSE 2014/2020; Dottorati innovativi con caratterizzazione industriale—PON R&I 2014–2020; “Sensore bio-elettronico usa-e-getta per l’HIV autoalimentato da una cella a combustibile biologica” (BioElSens&Fuel); SiMBiT—Single molecule bio-electronic smart system array for clinical testing (Grant agreement ID: 824946); PMGB—Sviluppo di piattaforme mecatroniche, genomiche e bioinformatiche per l’oncologia di precisione—ARS01_01195-PON “RICERCA E INNOVAZIONE” 2014–2020; Åbo Akademi University CoE “Bioelectronic activation of cell functions”; and CSGI are acknowledged for partial financial support.

CONFLICT OF INTEREST

The authors declare no conflict of interest.

AUTHOR CONTRIBUTIONS

All authors have thoroughly contributed to conceiving and writing this article. The final version was approved by all authors.

DATA AVAILABILITY STATEMENT

Not applicable.

ORCID

Paolo Bollella  <https://orcid.org/0000-0001-9049-6406>

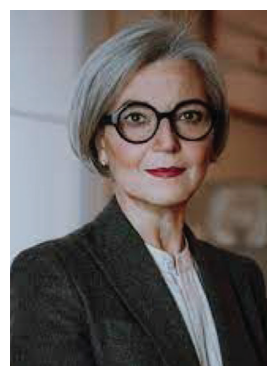
REFERENCES

1. K. Habermüller, M. Mosbach, W. Schuhmann, *Fresenius J. Anal. Chem.* **2000**, 366, 560.
2. N. L. Walker, A. B. Roshkolaeva, A. I. Chapoval, J. E. Dick, *Curr. Opin. Electrochem.* **2021**, 28, 100735.
3. A. A. Karyakin, O. V. Gitelmacher, E. E. Karyakina, *Anal. Chem.* **1995**, 67, 2419.
4. A. A. Karyakin, O. A. Bobrova, E. E. Karyakina, *J. Electroanal. Chem.* **1995**, 399, 179.
5. S. Abdellaoui, R. D. Milton, T. Quah, S. D. Minter, *Chem. Commun.* **2016**, 52, 1147.
6. P. Bollella, L. Gorton, *Curr. Opin. Electrochem.* **2018**, 10, 157.
7. P. Bollella, E. Katz, *Sensors* **2020**, 20, 3517.
8. P. Bollella, R. Ludwig, L. Gorton, *Appl. Mater. Today* **2017**, 9, 319.
9. L. C. Clark Jr, C. Lyons, *Ann. N. Y. Acad. Sci.* **1962**, 102, 29.
10. J. Wang, *Chem. Rev.* **2008**, 108, 814.
11. J. Wang, *Electroanalysis* **2001**, 13, 983.
12. S. D. Caras, D. Petelenz, J. Janata, *Anal. Chem.* **1985**, 57, 1920.
13. J. Janata, *Analyst* **1994**, 119, 2275.
14. J. Janata, S. D. Moss, *Biomed. Eng.* **1976**, 11, 241.
15. S. Caras, J. Janata, *Anal. Chem.* **1980**, 52, 1935.
16. J. T. Mabeck, G. G. Malliaras, *Anal. Bioanal. Chem.* **2006**, 384, 343.
17. C. Bartic, G. Borghs, *Anal. Bioanal. Chem.* **2006**, 384, 354.
18. M. J. Schöning, A. Poghossian, *Analyst* **2002**, 127, 1137.
19. M. J. Schöning, A. Poghossian, *Electroanalysis* **2006**, 18, 1893.
20. D. R. Thévenot, K. Toth, R. A. Durst, G. S. Wilson, *Biosens. Bioelectron.* **2001**, 16, 121.
21. P. Bergveld, *IEEE Trans. Biomed. Eng. BME-17*, **1970**, 70.
22. R. Kühnhold, H. Ryssel, *Sens. Actuators B Chem.* **2000**, 68, 307.
23. J. C. Chou, Y. S. Li, J. L. Chiang, *Sens. Actuators B Chem.* **2000**, 71, 73.
24. P. Bergveld, *Sens. Actuators* **1981**, 1, 17.
25. S. M. Sze, Y. Li, K. K. Ng, *Physics of Semiconductor Devices*, John Wiley & Sons **2021**.
26. M. K. Sarma, P. K. Sharma, J. Ch. Dutta, *Int. Conf. Electr. Electron. Optim. Tech.*, **2016**, 409.
27. A. Sibbald, *J. Mol. Electron.* **1986**, 2, 51.
28. P. Bergveld, A. Sibbald, *Analytical and Biomedical Applications of Ion-Selective Field-Effect Transistors*, Elsevier Science Limited **1988**.
29. B. H. van der Schoot, P. Bergveld, *Biosensors* **1987**, 3, 161.
30. L. K. Meixner, S. Koch, *Sens. Actuators B Chem.* **1992**, 6, 315.
31. I. Lundström, A. van den Berg, B. H. van der Schoot, H. H. van den Vlekkert, M. Armgarth, C. I. Nylander, *Sens. Chem. Biochem. Sens.* **1991**, 2, 467.
32. X.-L. Luo, J.-J. Xu, W. Zhao, H.-Y. Chen, *Sens. Actuators B Chem.* **2004**, 97, 249.
33. A. P. Soldatkin, J. Montoriol, W. Sant, C. Martelet, N. Jaffrezic-Renault, *Talanta* **2002**, 58, 351.
34. A. Poghossian, T. Yoshinobu, A. Simonis, H. Ecken, H. Lüth, M. J. Schöning, *Sens. Actuators B Chem.* **2001**, 78, 237.
35. B. Danielsson, I. Lundström, K. Mosbach, L. Stibler, *Anal. Lett.* **1979**, 12, 1189.

36. S. V. Dzyadevych, A. P. Soldatkin, Y. I. Korpan, V. N. Arkhypova, V. Anna, J.-M. Chovelon, C. Martelet, N. Jaffrezic-Renault, *Anal. Bioanal. Chem.* **2003**, *377*, 496.
37. A. Poghosian, M. J. Schöning, P. Schroth, A. Simonis, H. Lüth, *Sens. Actuators B Chem.* **2001**, *76*, 519.
38. A. Poghosian, M. J. Schöning, *Electroanalysis* **2004**, *16*, 1863.
39. A. A. Shul'ga, M. Koudelka-Hep, N. F. de Rooij, L. I. Netchiporouk, *Anal. Chem.* **1994**, *66*, 205.
40. R. Wilson, A. P. F. Turner, *Biosens. Bioelectron.* **1992**, *7*, 165.
41. G. S. Wilson, *Biosens. Bioelectron.* **2016**, *82*, vii.
42. P. N. Bartlett, F. A. Al-Lolage, *J. Electroanal. Chem.* **2018**, *819*, 26.
43. Y. Hanazato, S. Shiono, M. Maeda, *Anal. Chim. Acta* **1990**, *231*, 213.
44. D. G. Pijanowska, W. Torbic, *Sens. Actuators B Chem.* **1997**, *44*, 370.
45. A. B. Kharitonov, M. Zayats, L. Alfonta, E. Katz, I. Willner, *Sens. Actuators B Chem.* **2001**, *76*, 203.
46. A. B. Kharitonov, J. Wasserman, E. Katz, I. Willner, *J. Phys. Chem. B* **2001**, *105*, 4205.
47. J. Mocak, A. M. Bond, S. Mitchell, G. Scollary, *Pure Appl. Chem.* **1997**, *69*, 297.
48. S. P. Pogorelova, M. Zayats, A. B. Kharitonov, E. Katz, I. Willner, *Sens. Actuators B Chem.* **2003**, *89*, 40.
49. C.-S. Lee, S. K. Kim, M. Kim, *Sensors* **2009**, *9*, 7111.
50. A. Amine, H. Mohammadi, I. Bourais, G. Palleschi, *Biosens. Bioelectron.* **2006**, *21*, 1405.
51. M. Pohanka, K. Musilek, K. Kuca, *Curr. Med. Chem.* **2009**, *16*, 1790.
52. A. N. Hendji, N. Jaffrezic-Renault, C. Martelet, P. Clechet, A. A. Shlu'ga, V. I. Strikha, L. I. Netchiporuk, A. P. Soldatkin, W. B. Wlodarski, *Anal. Chim. Acta* **1993**, *281*, 3.
53. T. Kullick, M. Beyer, J. Henning, T. Lerch, R. Quack, A. Zeitz, B. Hitzmann, T. Scheper, K. Schürgerl, *Anal. Chim. Acta* **1994**, *296*, 263.
54. J. Van der Spiegel, I. Lauks, P. Chan, D. Babic, *Sens. Actuators* **1983**, *4*, 291.
55. S. A. Pullano, C. D. Critello, I. Mahbub, N. T. Tasneem, S. Shamsir, S. K. Islam, M. Greco, A. S. Fiorillo, *Sensors* **2018**, *18*, 4042.
56. J.-K. Park, W.-J. Cho, *Appl. Phys. Lett.* **2012**, *101*, art. No. 133703.
57. P.-C. Yao, J.-L. Chiang, M.-C. Lee, *Solid State Sci.* **2014**, *28*, 47–54.
58. K. Singh, B.-S. Lou, J.-L. Her, S.-T. Pang, T.-M. Pan, *Sens. Actuators B Chem.* **2019**, *298*, art. No. 126837.
59. H.-J. Jang, J.-G. Gu, W.-J. Cho, *Sens. Actuators B Chem.* **2013**, *181*, 880.
60. S.-P. Chang, T.-H. Yang, *Int J Electrochem Sci* **2012**, *7*, 50207.
61. P. Bollella, E. Katz, *Methods Enzymol.* **2020**, *630*, 215.
62. E. Dilonardo, M. Penza, M. Alvisi, C. Di Franco, R. Rossi, F. Palmisano, L. Torsi, N. Cioffi, *Sens. Actuators B Chem.* **2016**, *223*, 417.
63. N. Iqbal, A. Afzal, N. Cioffi, L. Sabbatini, L. Torsi, *Sens. Actuators B Chem.* **2013**, *181*, 9–21.
64. N. Cioffi, L. Colaiani, E. Ieva, R. Pilolli, N. Ditaranto, M. D. Angione, S. Cotrone, K. Buchholt, A. L. Spetz, L. Sabbatini, *Electrochimica Acta* **2011**, *56*, 3713.
65. M. Izzi, M. C. Sportelli, L. Tursellino, G. Palazzo, R. A. Picca, N. Cioffi, Á. I. López Lorente, *Nanomaterials* **2020**, *10*, 622.
66. P. Bollella, C. Schulz, G. Favero, F. Mazzei, R. Ludwig, L. Gorton, R. Antiochia, *Electroanalysis* **2017**, *29*, 77.
67. Q. Zhang, W. Liu, C. Sun, H. Zhang, W. Pang, D. Zhang, X. Duan, *Nanotechnology* **2015**, *26*, art. No. 355202.
68. J.-C. Lin, B.-R. Huang, Y.-K. Yang, *Sens. Actuators B Chem.* **2013**, *184*, 27–32.
69. N. C. Vieira, A. Figueiredo, A. D. Faceto, A. A. de Queiroz, V. Zucolotto, F. E. Guimarães, *Sens. Actuators B Chem.* **2012**, *169*, 397.
70. L.-T. Yin, J.-C. Chou, W.-Y. Chung, T.-P. Sun, S.-K. Hsiung, *Sens. Actuators B Chem.* **2000**, *71*, 106.
71. L.-L. Chi, J.-C. Chou, W.-Y. Chung, T.-P. Sun, S.-K. Hsiung, *Mater. Chem. Phys.* **2000**, *63*, 19.
72. Y.-L. Chin, J.-C. Chou, Z.-C. Lei, T.-P. Sun, W.-Y. Chung, S.-K. Hsiung, *Jpn. J. Appl. Phys.* **2001**, *40*, 6311–6315, art. No. 6311.
73. P. D. Batista, M. Mulato, C. O. de Graeff, F. J. R. Fernandez, F. das, C. Marques, *Braz. J. Phys.* **2006**, *36*, 478.
74. C. J. Chiu, S. P. Chang, S.-J. Chang, *IEEE Electron Device Lett.* **2010**, *31*, 1245.
75. Y.-H. Lin, C.-P. Chu, C.-F. Lin, H.-H. Liao, H.-H. Tsai, Y.-Z. Juang, *Biomed. Microdevices* **2015**, *17*, art. No. 111.
76. H. J. N. P. D. Mello, M. Mulato, *Biomed. Microdevices* **2020**, *22*, art. No. 22.
77. J.-C. Chen, J.-C. Chou, T.-P. Sun, S.-K. Hsiung, *Sens. Actuators B Chem.* **2003**, *91*, 180.
78. J.-C. Chou, J.-S. Chen, M.-S. Huang, Y.-H. Liao, C.-H. Lai, T.-Y. Wu, S.-J. Yan, *IEEE Sens. J.* **2016**, *16*, 5588.
79. J.-L. Wang, P.-Y. Yang, T.-Y. Hsieh, P.-C. Juan, *Jpn. J. Appl. Phys.* **2015**, *55*, art. No. 01AE16.
80. S. A. Pullano, N. T. Tasneem, I. Mahbub, S. Shamsir, M. Greco, S. K. Islam, A. S. Fiorillo, *Sensors* **2019**, *19*, art. No. 1063.
81. M. Kamahori, Y. Ishige, M. Shimoda, *Biosens. Bioelectron.* **2007**, *22*, 3080.
82. S. Sasipongpana, Y. Rayanasukha, S. Prichanont, C. Thanachayanont, S. Porntheeraphat, N. Hounkanghang, *Mater. Today Proc.* **2017**, *4*, 6458.
83. L. Torsi, M. Magliulo, K. Manoli, G. Palazzo, *Chem. Soc. Rev.* **2013**, *42*, 8612.
84. H. Sirringhaus, *Adv. Mater.* **2014**, *26*, 1319.
85. M. Magliulo, K. Manoli, E. Macchia, G. Palazzo, L. Torsi, *Adv. Mater.* **2015**, *27*, 7528.
86. Y. Bonnassieux, C. J. Brabec, Y. Cao, T. B. Carmichael, M. L. Chabiny, K.-T. Cheng, G. Cho, A. Chung, C. L. Cobb, A. Distler, H.-J. Egelhaaf, G. Grau, X. Guo, G. Haghiashtiani, T.-C. Huang, M. M. Hussain, B. Iniguez, T.-M. Lee, L., Li, Y. Ma, D. Ma, M. C. McAlpine, T. N. Ng, R. Österbacka, S. N. Patel, J. Peng, H. Peng, J. Rivnay, L. Shao, D. Steingart, R. A. Street, V. Subramanian, L. Torsi, Y. Wu, *Flex. Print. Electron.* **2021**, *6*, 023001, art. No. 023001.
87. W. Brütting, *Physics of Organic Semiconductors*, John Wiley & Sons, Hoboken, NJ, **2005**.
88. S. Allard, M. Forster, B. Souharce, H. Thiem, U. Scherf, *Angew. Chem. Int. Ed.* **2008**, *47*, 4070.
89. L. Sabbatini, C. Malitesta, E. De Giglio, I. Losito, L. Torsi, P. G. Zambonin, *J. Electron Spectrosc. Relat. Phenom.* **1999**, *100*, 35.
90. L. Torsi, F. Marinelli, M. D. Angione, A. Dell'Aquila, N. Cioffi, E. De Giglio, L. Sabbatini, *Org. Electron.* **2009**, *10*, 233.

91. E. Macchia, P. Romele, K. Manoli, M. Ghittorelli, M. Magliulo, Z. M. Kovács-Vajna, F. Torricelli, L. Torsi, *Flex. Print. Electron.* **2018**, *3*, art. No. 034002.
92. S. K. Sailapu, E. Macchia, I. Merino-Jimenez, J. P. Esquivel, L. Sarcina, G. Scamarcio, S. D. Minter, L. Torsi, N. Sabaté, *Biosens. Bioelectron.* **2020**, *156*, 112103.
93. E. Macchia, K. Manoli, C. Di Franco, R. A. Picca, R. Österbacka, G. Palazzo, F. Torricelli, G. Scamarcio, L. Torsi, *ACS Sens.* **2020**, *5*, 1822.
94. E. Macchia, K. Manoli, B. Holzer, C. Di Franco, M. Ghittorelli, F. Torricelli, D. Alberga, G. F. Mangiatordi, G. Palazzo, G. Scamarcio, L. Torsi, *Nat. Commun.* **2018**, *9*, art. No. 3223.
95. E. Macchia, R. A. Picca, K. Manoli, C. Di Franco, D. Blasi, L. Sarcina, N. Ditaranto, N. Cioffi, R. Österbacka, G. Scamarcio, F. Torricelli, L. Torsi, *Mater. Horiz.* **2020**, *7*, 999.
96. R. A. Picca, K. Manoli, E. Macchia, L. Sarcina, C. Di Franco, N. Cioffi, D. Blasi, R. Österbacka, F. Torricelli, G. Scamarcio, L. Torsi, *Adv. Funct. Mater.* **2020**, *30*, art. No. 1904513.
97. E. Macchia, A. Tiwari, K. Manoli, B. Holzer, N. Ditaranto, R. A. Picca, N. Cioffi, C. Di Franco, G. Scamarcio, G. Palazzo, L. Torsi, *Chem. Mater.* **2019**, *31*, 6476–6483.
98. M. Magliulo, D. De Tullio, I. Vikholm-Lundin, W. M. Albers, T. Munter, K. Manoli, G. Palazzo, L. Torsi, *Anal. Bioanal. Chem.* **2016**, *408*, 3943.
99. E. Macchia, K. Manoli, B. Holzer, C. Di Franco, R. A. Picca, N. Cioffi, G. Scamarcio, G. Palazzo, L. Torsi, *Anal. Bioanal. Chem.* **2019**, *411*, 4899.
100. P. Lin, F. Yan, J. Yu, H. L. Chan, M. Yang, *Adv. Mater.* **2010**, *22*, 3655.
101. P. Romele, M. Ghittorelli, Z. M. Kovács-Vajna, F. Torricelli, *Nat. Commun.* **2019**, *10*, art. No. 3044.
102. K. Guo, S. Wustoni, A. Koklu, E. Díaz-Galicia, M. Moser, A. Hama, A. A. Alqahtani, A. N. Ahmad, F. S. Alhamlan, M. Shuaib, A. Pain, I. McCulloch, S. T. Arold, R. Grünberg, S. Inal, *Nat. Biomed. Eng.* **2021**, *5*, 666.
103. D. A. Bernards, D. J. Macaya, M. Nikolou, J. A. DeFranco, S. Takamatsu, G. G. Malliaras, *J. Mater. Chem.* **2008**, *18*, 116.
104. T. Minami, T. Minami, Y. Sasaki, R. Kurita, O. Niwa, S. Wakida, S. Tokito, *Anal. Sci.* **2015**, *31*, 725.
105. E. Bihar, Y. Deng, T. Miyake, M. Saadaoui, G. G. Malliaras, M. Rolandi, *Sci. Rep.* **2016**, *6*, art. No. 27582.
106. A. -M. Pappa, O. Parlak, G. Scheiblin, P. Mailley, A. Salleo, R. M. Owens, *Trends Biotechnol.* **2018**, *36*, 45.
107. T. Minami, Y. Sasaki, T. Minamiki, P. Koutnik, P. Anzenbacher, S. Tokito, *Chem. Commun.* **2015**, *51*, 17666.
108. T. Minami, T. Minamiki, Y. Hashima, D. Yokoyama, T. Sekine, K. Fukuda, D. Kumaki, S. Tokito, *Chem. Commun.* **2014**, *50*, 15613.
109. Z.-T. Zhu, J. T. Mabeck, C. Zhu, N. C. Cady, C. A. Batt, G. G. Malliaras, *Chem. Commun.* **2004**, *13*, 1556.
110. C. H. Mak, C. Liao, Y. Fu, M. Zhang, C. Y. Tang, Y. H. Tsang, H. L. Chan, F. Yan, *J. Mater. Chem. C* **2015**, *3*, 6532.
111. X. Strakosas, M. Huerta, M. J. Donahue, A. Hama, A. -M. Pappa, M. Ferro, M. Ramuz, J. Rivnay, R. M. Owens, *J. Appl. Polym. Sci.* **2017**, *134*, art. No. 44483.
112. T. Minami, T. Sato, T. Minamiki, K. Fukuda, D. Kumaki, S. Tokito, *Biosens. Bioelectron.* **2015**, *74*, 45.
113. T. Minamiki, S. Tokito, T. Minami, *Anal. Sci.* **2018**, *35*, 103.
114. P. Didier, T. Minami, *Semicond. Sci. Technol.* **2020**, *35*, art. No. 11LT02.
115. T. Minami, T. Sato, T. Minamiki, S. Tokito, *Anal. Sci.* **2015**, *31*, 721.
116. J. Lange, C. Wittmann, *Anal. Bioanal. Chem.* **2002**, *372*, 276–283.
117. M. Di Fusco, R. Federico, A. Boffi, A. Macone, G. Favero, F. Mazzei, *Anal. Bioanal. Chem.* **2011**, *401*, 707.
118. S. K. Kannan, B. Ambrose, S. Sudalaimani, M. Pandiaraj, K. Giribabu, M. Kathiresan, *Anal. Methods* **2020**, *12*, 3438.
119. T. Minami, Y. Sasaki, T. Minamiki, S. Wakida, R. Kurita, O. Niwa, S. Tokito, *Biosens. Bioelectron.* **2016**, *81*, 87.
120. K. Nagamine, A. Nomura, Y. Ichimura, R. Izawa, S. Sasaki, H. Furusawa, H. Matsui, S. Tokito, *Anal. Sci.* **2020**, *36*, 291.
121. R. Shiwaku, H. Matsui, K. Nagamine, M. Uematsu, T. Mano, Y. Maruyama, A. Nomura, K. Tsuchiya, K. Hayasaka, Y. Takeda, *Sci. Rep.* **2018**, *8*, art. No. 3922.
122. H. Furusawa, Y. Ichimura, K. Nagamine, R. Shiwaku, H. Matsui, S. Tokito, *Technologies* **2018**, *6*, 77, art. No. 77.
123. Y. Sun, M. Luo, X. Meng, J. Xiang, L. Wang, Q. Ren, S. Guo, *Anal. Chem.* **2017**, *89*, 3761.
124. C. Sun, X. Wang, M. A. Auwalu, S. Cheng, W. Hu, *EcoMat* **2021**, *3*, art. No. e12094.
125. Y. -C. Syu, W. -E. Hsu, C. -T. Lin, *ECS J. Solid State Sci. Technol.* **2018**, *7*, Q3196.
126. D. Ohayon, G. Nikiforidis, A. Savva, A. Giugni, S. Wustoni, T. Palanisamy, X. Chen, I. P. Maria, E. Di Fabrizio, P. M. Costa, *Nat. Mater.* **2020**, *19*, 456.
127. P. Bollella, L. Gorton, R. Antiochia, *Sensors* **2018**, *18*, art. No. 1319.
128. T. Adachi, Y. Kitazumi, O. Shirai, K. Kano, *Catalysts* **2020**, *10*, art. No. 236.
129. P. Bollella, S. Edwardraja, Z. Guo, Kirill Alexandrov, E. Katz, *J. Phys. Chem. Lett.* **2020**, *11*, 5549.
130. P. Bollella, S. Edwardraja, Z. Guo, C. E. Vickers, J. Whitfield, P. Walden, A. Melman, K. Alexandrov, E. Katz, *ACS Sens.* **2021**, *6*, 3596.

AUTHOR BIOGRAPHIES



Luisa Torsi is a Professor of chemistry at the University of Bari and an adjunct professor at Abo Academy University. She received her *Laurea* degree in Physics and the Ph.D. in Chemical Sciences from UNIBA and was a post-doctoral fellow at Bell Labs in the USA. She was the first woman

awarded the H.E. Merck prize. She was also awarded the Distinguished Women Award by the International Union of Pure and Applied Chemistry. Lately, she was awarded also the Wilhelm Exner Medal 2021. Torsi has authored more than 200 ISI papers, including papers published in *Science*, *Nature Materials*. Her works gathered almost 14,000 Google scholar citations result-

ing in an h-index of 56. Gathered research funding for over 26 M€, comprises several European and national contracts. Torsi is committed to the role-modeling for younger women scientists. In a recent campaign she was featured in a story of TOPOLINO (Italian comic digest-size series of Disney comics), as “Louise Torduck”, a successful female scientist of the Calisota valley.



Paolo Bollella is an Assistant Professor at the University of Bari in the Department of Chemistry. Till December 2020, he was a Research Assistant Professor at Clarkson University in the Department of Chemistry and Biomolecular Science (USA). After his Ph.D., he joined the Department of Analytical Chemistry at Åbo Akademi in Turku (Finland) with a Johan Gadolin PostDoc fellowship awarded from the board of Johan Gadolin Process Chemistry Center. In October 2018, he joined the group of “Bioelectronics &

Bionanotechnology” led by Prof. Evgeny Katz. In March 2019, he was awarded the Minerva Prize for the Scientific Research – Merit Mention for the achievements obtained during his doctoral thesis based on the study of Mediated/Direct Electron Transfer of Redox Protein for Biosensors and Biofuel Cells Applications. In 2020, he was recognized among the top 100,000 most influencing scientists and engineers (statistical analysis elaborated by Stanford University). He is the author of 72 papers on peer-reviewed international journals (Hirsch-index 20), three book chapters, one student book, two proceedings, and almost 60 oral or poster contributions to national and international conferences.

How to cite this article: L. Sarcina, E. Macchia, A. Tricase, C. Scandurra, A. Imbriano, F. Torricelli, N. Cioffi, L. Torsi, P. Bollella. *Electrochem. Sci. Adv.* **2023**, *3*, e2100216.

<https://doi.org/10.1002/elsa.202100216>